Oceanological and Hydrobiological Studies

International Journal of Oceanography and Hydrobiology

Volume 50, No. 1, March 2021

pages (98-114)

sciendo

ISSN 1730-413X
eISSN 1897-3191

Spatio-temporal variation of microphytoplankton communities in Obhur Creek, the central Red Sea

by

Mohsen M. El-Sherbiny[1,2,*],
Mamdouh A. Al-Harbi[1],
Anand J. Kumar[1]

DOI: **10.2478/oandhs-2021-0010**
Category: **Original research paper**
Received: **August 15, 2020**
Accepted: **October 22, 2020**

[1]Department of Marine Biology, Faculty of Marine Science, King Abdulaziz University, Jeddah 21589, Saudi Arabia

[2]Department of Marine Sciences, Faculty of Science, Suez Canal University, Ismailia 41522, Egypt

Abstract

The abundance and distribution of microphytoplankton and related physicochemical factors were assessed monthly in Obhur Creek, the central Red Sea. Sampling was carried out near the entrance, the middle and end parts of the creek. During the course of the present study, the Red Sea was characterized by predominantly oligotrophic conditions. Nutrient concentrations were relatively higher in the end part of the creek compared to the two other study sites. Chlorophyll *a* was also low throughout the year (average: 0.35 ± 0.32 mg m^{-3}), except in May when it showed clear peaks at open-water and middle sites of the creek (1.85 and 1.04 mg m^{-3}, respectively). Phytoplankton abundance followed a similar pattern to that of chlorophyll *a* with considerably higher abundance at these sites in May (3063.27×10^3 and 1082.34×10^3 individuals m^{-3}, respectively). This unusually higher abundance was mostly due to the proliferation of the diatom *Pseudo-nitzschia* cf. *delicatissima* (Cleve) Heiden. Silicate concentrations were statistically significantly correlated with total phytoplankton. A total of 220 phytoplankton species were recorded during the study period (117 diatoms, 99 dinoflagellates and four cyanophytes). Diatoms dominated in the phytoplankton abundance (75%) and were followed by dinoflagellates (20%), while cyanophytes accounted for a minimal proportion. Of all phytoplankton species observed during the study, 21 diatom and four dinoflagellate species were considered as new records for the Red Sea, and two diatom and 14 dinoflagellate species were listed as harmful algal species worldwide.

Key words: phytoplankton, abundance, distribution, Obhur Creek, Red Sea

---

* Corresponding author: ooomar@kau.edu.sa

online at www.oandhs.ug.edu.pl

1. Introduction

Environmental changes affect marine ecosystems around the world at an alarming rate. It is necessary to understand the consequences of these changes for different aspects of marine ecosystems (Halpern et al. 2008; Brierley & Kingsford 2009). The Red Sea is affected by natural and anthropogenic changes and is undergoing large-scale modifications, mainly along the coastal habitats (Peña-García et al. 2014). The coastal water conditions of the central Red Sea are changing from previously oligotrophic to mesotrophic and partially eutrophic (El-Sayed 2002; Mudarris & Turki 2006; Al-Farawati 2010; Peña-García et al. 2014). In general, the lack of rainfall and riverine inputs affects the supply of nutrients to the Red Sea (Edwards 1987), but increasing urbanization and industrialization compensate for this shortage at least in the coastal habitats of major metropolises, like Jeddah (Peña-García et al. 2014). Phytoplankton are the basis of the aquatic food web and therefore a detailed analysis of their ecology and population dynamics is crucial for elucidating vital information regarding ecosystem health, especially with increasing human interference in the ecosystem. Changes in environmental factors of the coastal waters of the central Red Sea exert a conspicuous influence on primary producers which often respond to these changes through either an increase or decrease in their population size (Al-Harbi & Affan 2016; Devassy et al. 2017; Al-Aidaroos et al. 2019; Al-Amri et al. 2020). Continuous monitoring of the coastal waters is therefore essential as it can provide further insights into changes associated with predicted environmental changes globally (Bastos et al. 2016).

There are limited studies related to the composition of microphytoplankton communities on the Saudi coast of the Red Sea and some of them focused only on a single station in Jeddah coastal waters (Dowidar 1983; Sheikh et al. 1986). In addition, phytoplankton communities in Obhur Creek were investigated for five months by Dowidar et al. (1978), whereas Touliabah et al. (2010) provided information on the seasonal variation of microphytoplankton communities in different lagoons located on the Jeddah coast. Recent research on the latitudinal distribution of microphytoplankton in coastal waters (Kürten et al. 2015), in the northern Red Sea (Devassy et al. 2017) and the central Red Sea (Al-Amri et al. 2020) has succeeded in adding relevant information on the phytoplankton community from this less explored ocean region.

The present study was carried out in Obhur Creek on the Saudi coast of the central Red Sea. The area is a tourist hotspot that is visited by a considerable number of tourists every year. It provides mooring services for vessels and offers recreational activities. The creek is described as a 9.2 km long natural cut in the coralline limestone of the Tihama coastal plain, which opens at the southwestern end of the Red Sea through a narrow, 264 m wide outlet (Basaham & El-Sayed 2006). It has a depth of about 50 m at the mouth, which gradually decreases toward its northeastern extremity to become less than 6 m deep at the end part (Basaham & El-Shater 1994). Due to the extensive renovation processes in terms of building resorts occurring along the banks of the creek, it is estimated that the water body has already lost 788 729 m^2 of its total area (Basaham & El-Sayed 2006).

This study is the first to show monthly changes in the structure of phytoplankton communities and their interactions with other environmental factors within the creek as well as in the Saudi coastal waters of the Red Sea. It also gives a brief account of harmful diatom and dinoflagellate species in this region.

2. Materials and methods

2.1. Sampling sites

In this study, three sites were selected for monthly sampling within the creek. Site 1 (reference site) was 2 km away from the creek mouth toward the open waters and is expected to be away from any source of anthropogenic impact. It has an average depth of about 200 m and shows typical characteristics of the Red Sea coastal waters. Site 2 was located in the middle zone of the creek and receives discharges from an aquaculture facility. Site 3 was located at the northeastern end of the creek, exposed to human disturbance, and was characterized by shallow waters and weak water exchange (Fig. 1).

2.2. Sampling and analysis

Monthly phytoplankton and surface seawater samples were collected from January through December (2017). The sampling was carried out during daytime using a mechanized boat. Salinity and temperature were measured in situ using a water quality probe (Horiba U50). A Niskin sampler (Hydrobios – 5 l) was used to collect 10 l of seawater from a depth of 0.5 m in order to measure inorganic nutrients and phytoplankton biomass (chlorophyll *a*). To determine chlorophyll *a*, 3–5 l of seawater was filtered through a Whatman GF/F filter paper (0.7 μm, 47 mm) and kept at –80°C until further analysis. To estimate inorganic nutrient concentrations, 500 ml of seawater was filtered

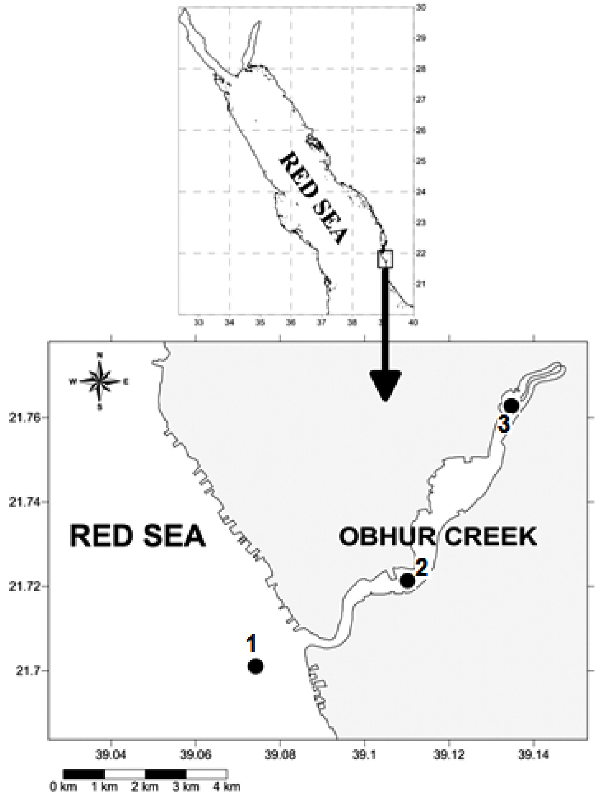

Figure 1

Location of the study sites

through a Whatman Nucleopore membrane filter (0.2 µm). The analysis of both chlorophyll *a* and inorganic nutrients (nitrate, nitrite, ammonia, phosphate and silicate) was carried out according to the protocols by Parsons et al. (1984) using a UV spectrophotometer (Shimadzu UV 1700).

A phytoplankton net (Hydrobios) with a mesh size of 20 µm was used for sampling. The net was fitted with a flowmeter to calculate the volume of filtered water (VWF) based on this equation:

$$VWF = \pi r^2 \times d$$

where "r" is the radius of the net and "d" is the haul distance, which is obtained as the difference between initial and final flowmeter readings. The net was towed horizontally for 6–10 min at a boat speed of ~1 knot. The collected samples were then immediately fixed with Lugol's iodine solution and a few drops of concentrated formaldehyde solution (Kürten et al. 2015). Prior to analysis, samples were screened through a 500 µm net to remove large particles of both biological and non-biological origin. A Sedgewick Rafter Counting Cell (1 ml/1 µl) was used to assess phytoplankton abundance under an inverted microscope (Leica DMI 3000B). The protocols provided by LeGresley & McDermott (2010) were followed for systematic analysis of phytoplankton abundance and a triplicate counting procedure was performed on each phytoplankton sample to increase the accuracy of the analysis. The counting method detailed in Devassy et al. (2019) was employed to determine the number of squares in Sedgewick-Rafter chamber. Phytoplankton species were taxonomically classified with the help of identification catalogues (Taylor 1976; Tomas 1997; Hallegraeff 2003; Gómez 2013) and then validated with the help of WoRMS (World Register of Marine Species; www.marinespecies.org) and named according to the latest taxonomical nomenclature.

2.3. Statistical analysis

Relationships between physicochemical variables and phytoplankton biomass and abundance were determined using Pearson's correlation coefficient *r* (SPSS V23). One-way analysis of variance (ANOVA) was performed to determine spatial and temporal variations of different parameters using SPSS V23. Species richness, Shannon–Wiener index (*H'*) and evenness (*J'*) as well as the Bray–Curtis Similarity Index were computed using PRIMER 6 (Clarke & Gorley 2006). Prior to analysis, the data were square root transformed due to the apparent deviation from the normal distribution.

3. Results

3.1. Temperature and salinity

Spatial variation in temperature distribution was less pronounced, while significant temporal variation ($p < 0.01$) in salinity was observed during the study. Maximum temperature (32.2°C) and salinity (40.18) were recorded at site 3 in September, while the minimum values (24.5°C and 38.85) were recorded in March at sites 1 and 3, respectively (Fig. 2). Salinity values at site 1 were almost similar throughout the year, ranging between 38.85 and 39.52 in March and August, respectively (Fig. 2). Site 3 differed slightly and showed higher values (average: 39.53 ± 0.40) compared to the two other sites.

3.2. Inorganic nutrients

Nitrate concentrations (NO_3^-) ranged between a minimum of 0.03 µmol l^{-1} at site 2 in June and a maximum of 4.50 µmol l^{-1} at site 3 in August with

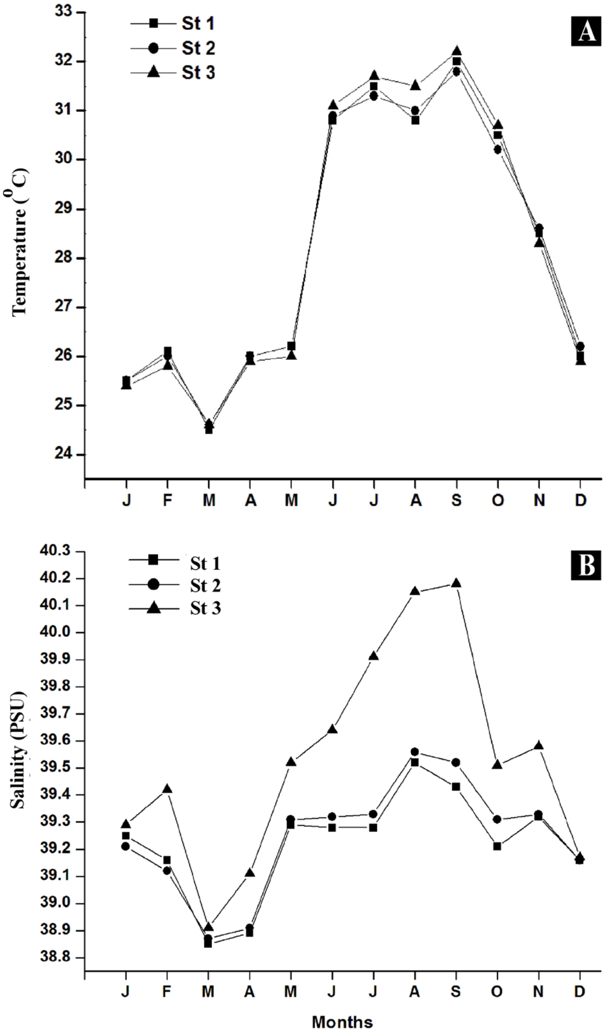

Figure 2

Monthly variations in: A) average temperature and B) salinity at different studied sites

an overall average of 0.73 ± 0.76 μmol l^{-1}. Although only slight variations in nitrate concentration were observed at sites 1 and 2 (mean values: 0.52 ± 0.60 and 0.34 ± 0.23 μmol l^{-1}, respectively), site 3 showed higher nitrate concentration (average: 1.32 ± 1.41 μmol l^{-1}; Fig. 3a). Higher nitrate values were observed at site 3 between August and November (Fig. 3a), with a maximum of 4.50 μmol l^{-1} in August. Nitrite (NO_2^-) values ranged from 0.01 to 0.22 μmol l^{-1} at site 1 (August) and site 3 (September), respectively (Fig. 3b). On the other hand, ammonia (NH_4^+) showed significant variations among the sites. Higher ammonia concentration was observed at site 3 (average: 1.48 ± 1.31 μmol l^{-1}) followed by sites 2 and 1 (mean values: 1.04 ± 0.99 μmol l^{-1} and 0.36 ± 0.21 μmol l^{-1}, respectively). Similar to nitrate, ammonia values also showed an increasing trend toward the second half of the year in the study region (Fig. 3c). Phosphate (PO_4^{3-}) ranged between 0.01 and 0.33 μmol l^{-1} with an average of 0.08 ± 0.08 μmol l^{-1} and no spatial variation was detected. Higher phosphate concentrations were observed between February and April with a maximum average value of 0.25 ± 0.07 μmol l^{-1} in March (Fig. 3d). Silicate concentration varied significantly among the sites, with relatively higher values at site 3 (average: 2.38 ± 0.38 μmol l^{-1}) compared to the other sites (Fig. 3e).

3.3. Chlorophyll *a*

Chlorophyll *a* concentration was generally low throughout the study region (average: 0.35 ± 0.32 mg m^{-3}) with a pattern similar to the distribution of nutrients, except a few cases (Fig. 3f). Chlorophyll *a* concentrations were relatively similar at sites 1 and 2 (mean values: 0.39 ± 0.48 and 0.40 ± 0.27 mg m^{-3}, respectively), though site 3 recorded the lowest mean value (0.26 ± 0.22 mg m^{-3}). The highest chlorophyll concentration (1.85 mg m^{-3}) was determined at site 1 in May, while the lowest value (0.015 mg m^{-3}) was recorded at site 3 in May. Chlorophyll values ranged between 0.05 and 1.85 mg m^{-3} at site 1 in April and May, respectively, between 0.05 and 1.04 mg m^{-3} at site 2 in January and May, respectively, and between 0.015 and 0.85 mg m^{-3} at site 3 in May and December, respectively (Fig. 3f).

3.4. Phytoplankton community composition

Diatoms were by far the most abundant group in the phytoplankton communities, accounting for 14.1 to 97% of the total phytoplankton throughout the year (mean: 75%). Dinoflagellates and cyanophytes, accounting for 20% (2.6–85.7%) and 5% (0.1–45.1%) of the total phytoplankton, ranked second and third in the abundance, respectively. Phytoplankton community composition was characterized by high diversity during the study period, with a total of 220 species (Supplementary material 1). Of the 220 phytoplankton species, 117 belonged to diatoms (76 Centrales and 41 Pennales), 99 to dinoflagellates and four species to cyanophytes. The maximum number of species (174) was found at site 2, which was followed by site 1 (170) and site 3 (128). Sites 1 and 2 were characterized by approximately similar diversity, with 84 diatoms and 81 dinoflagellates at the former (site 1) and 94 diatoms and 76 dinoflagellates at the latter (site 2) observed throughout the study period. Site 3 was less diverse than the two other sites, with 62 diatom and 64 dinoflagellate species (Supplementary

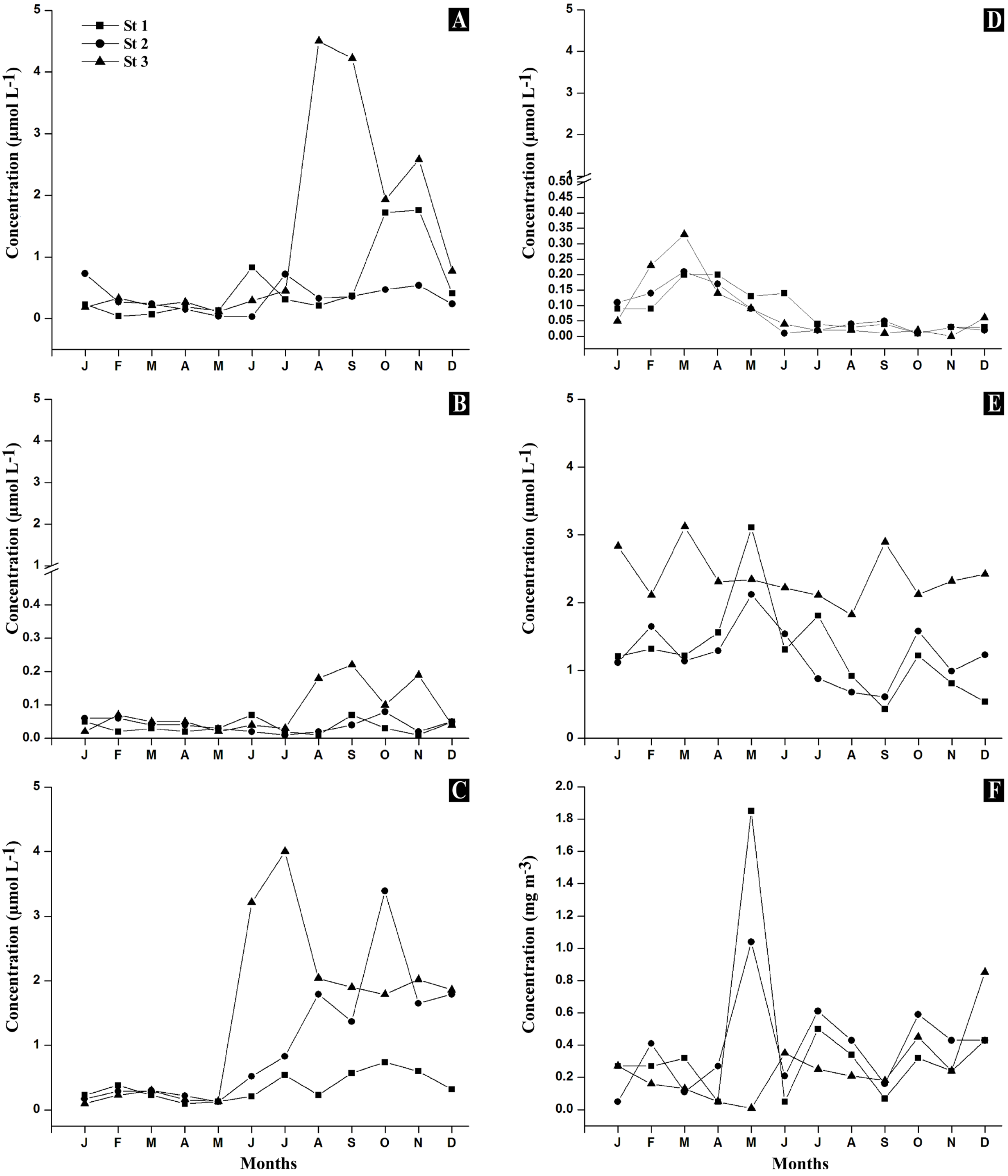

Figure 3

Chemical and biological parameters obtained from different sites during the study period: A) nitrate, B) nitrite, C) ammonia, D) phosphate, E) silicate and F) chlorophyll *a* material 1). Four Cyanophyta species were recorded at site 2 and only two species were found at sites 1 and 3, with the dominance of *Trichodesmium* sp., which accounted for 89.9% of the total cyanophytes. Centric diatoms were more dominant than pennates throughout the study period. Of the total phytoplankton species (220) observed, 21 diatoms and four dinoflagellate species are new records for the Red Sea. In addition, two diatoms (including *Pseudo-nitzschia* cf. *delicatissima*) and 14 dinoflagellates were listed on the IOC-UNESCO taxonomic reference list (Supplementary material 1) as potentially harmful species worldwide.

Rhizosolenia and *Chaetoceros* were the most diverse diatom genera in the current study (16 and 15 species, respectively). Other important diatom genera that contributed significantly to the diversity were: *Pleurosigma* (four species), *Cerataulina*, *Guinardia*, *Navicula* and *Nitzchia* (three species each; Supplementary material 1). Among dinoflagellates, the orders *Gonyaulacales* and *Peridiniales* were represented by the maximum number of genera (six genera), followed by *Dinophysiales* (three genera) and *Gymnodiniales* (two genera). The genus *Tripos* (synonym *Ceratium*) of dinoflagellates was observed with a maximum number of species (27 species), and was followed by *Protoperidinium* (18 species) and *Dinophysis* (nine species). At site 3, heterotrophic dinoflagellate species (33 species) dominated over the autotrophic ones and, for most of the study period, over diatoms. The most common dinoflagellate species occurring throughout the study period were: *Dinophysis caudata, D. tripos*, *Protoperidinium conicum*, *P. divergens*, *P. steinii*, *Tripos furca*, *T. fusus*, *T. horridus*, *T. lineatus* and *T. teres* (Supplementary material 1). On the other hand, the cyanophyte *Trichodesmium* sp. was recorded in relatively large numbers at sites 1 and 2 in June and July, and at site 3 in July.

3.5. Phytoplankton abundance

The abundance of phytoplankton in the study area varied between 7.95×10^3 and 3063.27 × 10^3 individuals m^{-3}, with an overall average of 238.59 × 10^3 ± 540.38 × 10^3 individuals m^{-3}. The highest average abundance of total phytoplankton was recorded at sites 1 and 2, with 295.72 × 10^3 ± 868.36 × 10^3 and 231.44 × 10^3 ± 306.98 × 10^3 individuals m^{-3}, respectively. On the other hand, the lowest average abundance was recorded at site 3 (139.81 × 10^3 ± 254.43 × 10^3 individuals m^{-3}). Regarding the monthly variation, a sharp peak in abundance was observed in May (average: 1389.63 × 10^3 ± 1543.12 × 10^3 individuals m^{-3}) due to the high density of *Pseudo-nitzschia* cf. *delicatissima* at sites 1 and 2 (2985.5 × 10^3 and 969.04 × 10^3 individuals m^{-3}, accounting for 97.5% and 89.5% of the total phytoplankton at these sites in May, respectively). Moreover, small increases were detected in July, October and December with average density of 256.62 × 10^3, 267.45 × 10^3 and 356.26 × 10^3 individuals m^{-3}, respectively. The total monthly phytoplankton abundance at site 1 varied between 7.95 × 10^3 individuals m^{-3} in September and 3063.27 × 10^3 individuals m^{-3} in May (Fig. 4a). At site 2, the abundance fluctuated between 14.48 × 10^3 and 1082.34 × 10^3 individuals m^{-3} in January and May, respectively (Fig. 4c). The abundance at site 3 ranged between 23.26 × 10^3 individuals m^{-3} in May and 929.34 × 10^3 individuals m^{-3} in December (Fig. 4e).

With an average abundance of 280.20 × 10^3 ± 861.17 individuals m^{-3} and a percentage contribution ranging from 21.05% in June to 98.36% in May, diatoms significantly dominated in the total phytoplankton abundance at site 1 for most of the study period. Dinoflagellates (average abundance: 24.27 × 10^3 ± 29.52 individuals m^{-3}), on the other hand, significantly dominated in the phytoplankton community at this site in August (64.91%) and September (52.50%). Cyanophytes (average abundance: 15.59 × 10^3 ± 43.17 individuals m^{-3}) dominated only in June and July, accounting for 60.15% and 46.55%, respectively. On the other hand, their contribution to the total abundance in the other months was almost negligible (Fig. 4b). Site 2 also showed a similar pattern of phytoplankton distribution as site 1, with diatoms (average abundance: 174.25 × 10^3 ± 290.93 individuals m^{-3}) being the most abundant group for most of the study period, except summer (July–September) when dinoflagellates (average abundance: 55.53 × 10^3 ± 52.45 individuals m^{-3}) dominated in the total phytoplankton abundance. Diatoms contributed 9.24% and 94.21% to the total abundance in July and May, respectively, while dinoflagellates contributed between 4.68% and 60.78% to the total abundance in May and September, respectively. Despite the presence of cyanophytes (average abundance: 17.02 × 10^3 ± 47.8 individuals m^{-3}) in summer (June–July), they were not the most abundant phytoplankton group (30.30 and 42.44%) in these particular months and showed negligible presence in the other ones (Fig. 4d). Site 3 differed from the two other sites in terms of the distribution of various phytoplankton groups and it was dominated by dinoflagellates (average abundance: 63.44 × 10^3 ± 69.67 individuals m^{-3}) for most of the study period, with a contribution ranging from

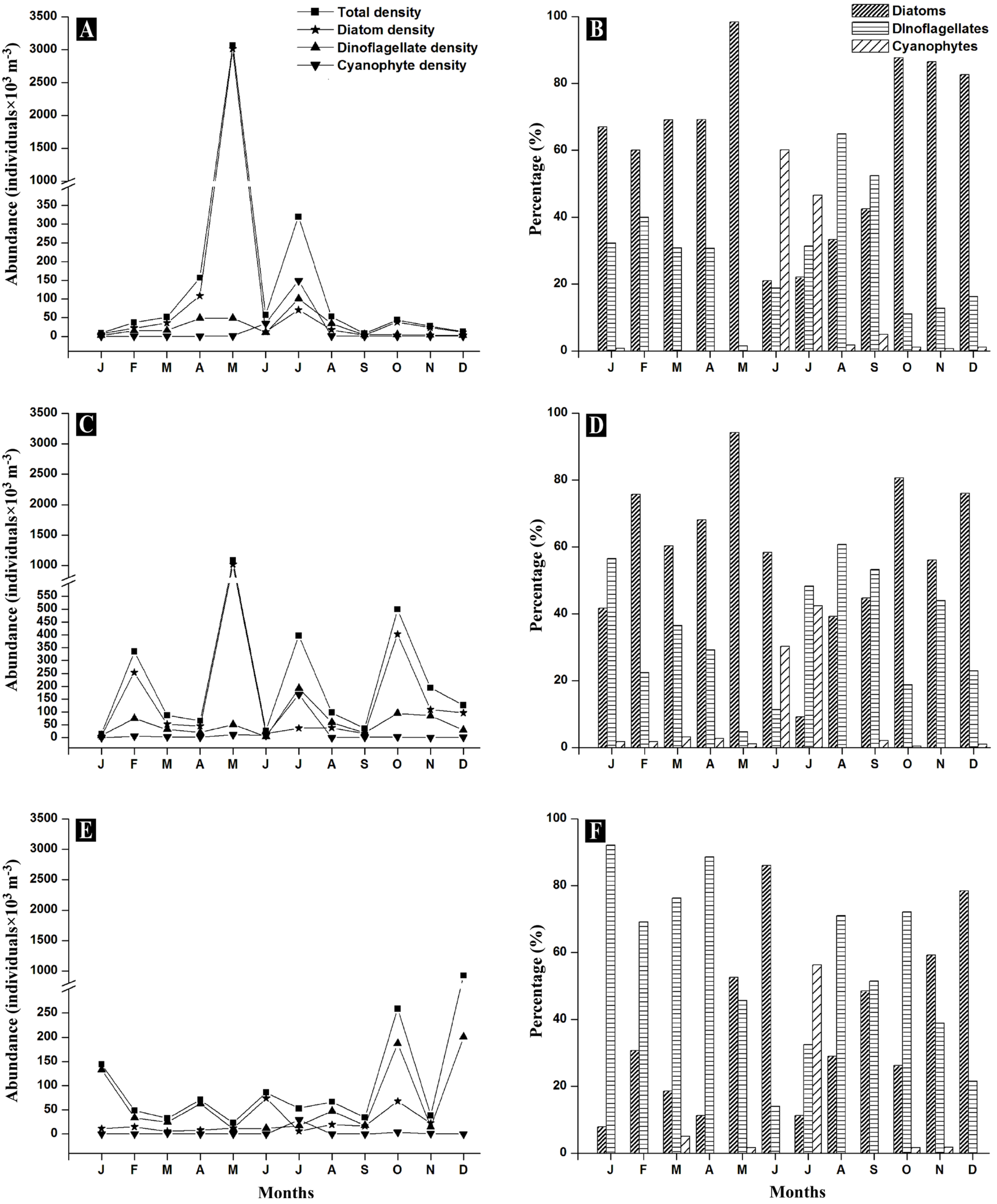

Figure 4

Variations in densities of total phytoplankton and different groups (A, C, E) along with the percentage contribution of each group to the total abundance (B, D, F) observed at site 1 (A, B), site 2 (C, D) and site 3 (E, F)

14% (June) to 92.08% (January). Diatoms (average abundance: $82.40 \times 10^3 \pm 204.97$ individuals m^{-3}) dominated in May–June and November–December and contributed from about 7.92% (January) to 86% (June) to the total phytoplankton abundance. Cyanophytes (average abundance: $3.07 \times 10^3 \pm 8.52$ individuals m^{-3}) dominated at this site (site 3) in July (56.25%) and were scarce in the other months (Fig. 4f).

3.6. Statistical analysis

Values of Pearson's coefficient of correlation (*r*) between individual parameters obtained in the study period showed a significant correlation for the total phytoplankton abundance with chlorophyll concentration ($p < 0.01$) as well as with silicate concentration ($p < 0.05$; Table 1). Physical parameters and nutrient salts showed a non-significant correlation with phytoplankton biomass and abundance. One-way analysis of variance (ANOVA) of salinity, nitrite, ammonia and silicate showed significant spatial variation, while temperature, salinity and phosphate showed significant temporal variation (Table 2). The dendrogram based on the Bray–Curtis similarity index of mean phytoplankton abundance showed a relatively high similarity between the sampling sites (> 60%). The similarity matrix of monthly phytoplankton abundance at each site also showed a roughly similar distribution pattern between the sites (Fig. 5). The dendrogram of site 1 (Fig. 5a) showed almost 78% similarity between the months except May, which was clearly separated from the others (35%). At site 2, the dendrogram indicated 63% similarity between the months (Fig. 5b). At site 3, on the other hand, all months showed 74% similarity except December (54%; Fig. 5c). Biodiversity indices clearly showed differences in the number of species. The lowest number of species was always recorded at site 3 (average: 28 ± 10), while sites 1 and 2 contained larger numbers (mean values: 44 ± 11 and 46 ± 17 at sites 1 and 2, respectively; Table 3). The Shannon–Wiener diversity index (*H'*) further confirmed differences in the diversity between the sites by providing relatively higher indices for site 1 (average: 3.75 ± 0.25) and 2 (average: 3.77 ± 0.35) compared to site 3 (average: 3.3 ± 0.32; Table 3). Relatively similar Pielou's evenness index (*J'*) revealed a uniform distribution of phytoplankton species at the study sites, with values ranging in a narrow range between 0.977 and 1.000 (Table 3).

4. Discussion

This study focuses on spatial and temporal changes in microphytoplankton biomass, community structure and abundance in relation to changing physical and chemical parameters. Increasing urbanization and the resulting anthropogenic impact induce certain changes in the relationships between biotic and abiotic factors of such a coastal ecosystem. The surface temperature values obtained during the study period are consistent with previous observations (Peña-García et al. 2014; Alsaafani et

Table 1

Values of Pearson's correlation coefficient (r) obtained for different environmental parameters observed during the study period (S – salinity, T – temperature, NO_3^- – nitrate, NO_2^- – nitrite, NH_4^+ – ammonia, PO_4^{3-} – phosphate, SiO_4^{4-} – silicate, Chl *a* – chlorophyll a and TPD – total phytoplankton abundance)

Parameters	S	T	NO_3^-	NO_2^-	NH_4^+	PO_4^{3-}	SiO_4^{4-}	Chl *a*	TPD
S	1								
T	.676**	1							
NO_3^-	.666**	.396*	1						
NO_2^-	.569**	0.232	.831**	1					
NH_4^+	.585**	.528**	.341*	.338*	1				
PO_4^{3-}	−.605**	−.661**	−.378*	−0.185	−.526**	1			
SiO_4^{4-}	0.188	−0.227	0.186	0.311	0.111	0.232	1		
Chl *a*	−0.036	−0.083	−0.132	−0.163	0.053	−0.133	0.273	1	
TPD	−0.069	−0.163	−0.138	−0.124	-0.073	0.052	.396*	.929**	1

** Correlation is significant at the 0.01 level (2-tailed).

* Correlation is significant at the 0.05 level (2-tailed).

Table 2

One-Way ANOVA obtained for different environmental parameters observed during the study period

Parameters	Between sites		Between months	
	F	Sig.	F	Sig.
Temperature	0.011	0.999	728.13	**0.001**
Salinity	4.552	**0.018**	4.336	**0.001**
Nitrate	3.214	0.053	1.155	0.366
Nitrite	4.531	**0.018**	0.68	0.743
Ammonia	4.205	0.024	1.591	0.165
Phosphate	0.063	0.939	10.413	**0.000**
Silicate	18.508	**0.000**	0.573	0.831
Chlorophyll *a*	0.585	0.563	1.91	**0.090**
Total phytoplankton density	0.291	0.75	1.853	0.1

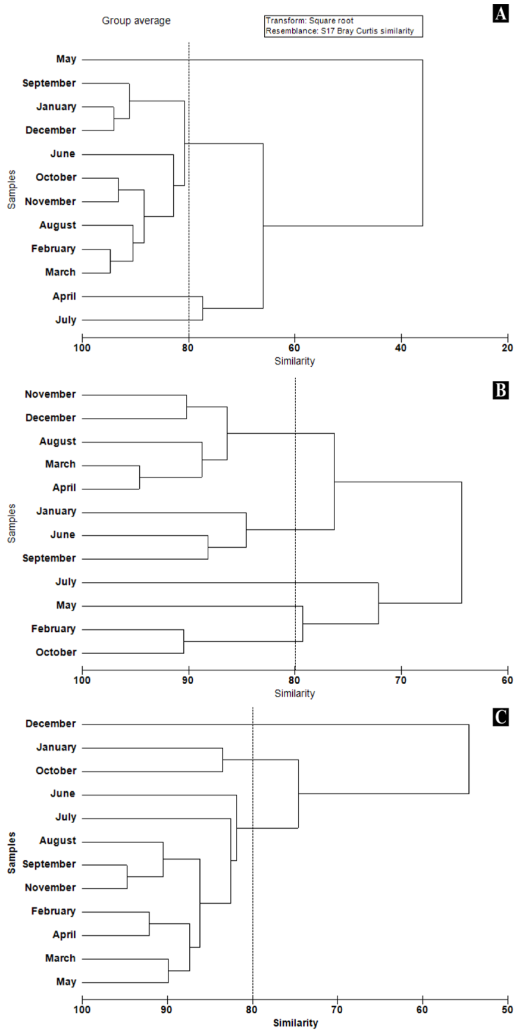

Figure 5

Dendrogram based on the Bray–Curtis similarity index revealing the pattern of phytoplankton abundance and distribution during the study period at three sites: A) site 1, B) site 2 and C) site 3

al. 2017). The area showed slight spatial variability in salinity, with the end part of the creek showing relatively higher values than the two other sites. This could be due to the good mixing of water at the entrance of the creek with water from the main Red Sea basin, eventually reaching the middle section and thus maintaining uniform salinity (Alsaafani et al. 2017). On the other hand, the decreasing depth from the entrance (50 m) toward the end part (6 m; Basaham & El-Sayed 2006) may also hinder the mixed-water column from reaching the end of the creek. The shallowness of the creek can also increase the evaporation rate in this hot and arid area, which may also eventually lead to higher surface salinity.

The distribution pattern of inorganic nutrients in the study area was similar to other coastal waters of the Red Sea (Peña-García et al. 2014; Qurban et al. 2014; Kürten et al. 2015; Wafar et al. 2016; Devassy et al. 2017; Al-Amri et al. 2020), with a few exceptions. Comparatively higher nutrient concentrations were observed at site 3 due to the lack of proper mixing, restricted water exchange and shallowness. Moreover, this site receives nutrient inputs mainly through wastewater from resorts and restaurants. A similar pattern of nutrient distribution from the creek was observed in April

Table 3

Biodiversity indices obtained for phytoplankton distribution at three sites, where S is the total number of species, *J′* is Pielou's evenness index and *H′* is the Shannon–Wiener diversity index

Month	Site 1			Site 2			Site 3		
	S	*J′*	*H′*	S	*J′*	*H′*	S	*J′*	*H′*
January	59	0.998	4.07	72	0.998	4.27	32	0.998	3.46
February	29	0.998	3.36	79	0.999	4.37	23	0.999	3.13
March	35	0.999	3.55	40	0.999	3.69	32	0.999	3.46
April	39	0.999	3.66	38	0.999	3.64	19	0.999	2.94
May	63	0.998	4.14	31	0.998	3.43	20	0.998	2.99
June	44	0.998	3.78	30	0.996	3.39	30	0.998	3.39
July	53	0.998	3.96	57	0.998	4.04	27	0.998	3.29
August	44	1.000	3.78	33	0.999	3.49	26	1.000	3.26
September	33	0.999	3.49	36	1.000	3.58	17	0.999	2.83
October	43	0.997	3.75	50	0.999	3.91	38	0.999	3.64
November	54	0.998	3.98	61	0.999	4.11	55	0.999	4.00
December	32	1.000	3.46	29	0.999	3.36	24	0.997	3.17

and October by Peña-García et al. (2014). Apart from site 3, nitrogen derivatives were relatively high at site 2 toward the second half of the year (June–December). This may be attributed to the discharge from the aquaculture facility, which operates at its maximum between June and December. A similar trend of increasing nutrient concentrations after summer was observed in previous studies in the coastal waters of Jeddah (El-Sayed 2002; Al-Farawati 2010; Peña-García et al. 2014).

Chlorophyll *a* clearly followed the pattern of nutrient distribution. A clear peak was observed in May along with some slight increases in July, October and December. These random peaks are common on the Red Sea coasts and occur mainly during the summer season (Acker et al. 2008; Racault et al. 2015; Devassy et al. 2017; Li et al. 2017). Apart from the peaks, the values were low, reflecting the oligotrophic nature of the Red Sea as stated in other studies (Qurban et al. 2014; Kürten et al. 2015; 2016). The observed peak was mainly due to the proliferation of the pennate diatom (*Pseudo-nitzschia* cf. *delicatissima*). The availability of surplus nutrients along with favorable water temperature may result in potential outbreaks of this species. Compared to the two other sites, site 3 was characterized by lower chlorophyll values throughout the study period despite having sufficient nutrients. The lower depths, which in turn makes the water column continuously turbid, create unfavorable conditions for phytoplankton growth.

Phytoplankton abundance showed spatial and temporal differences in the study area, with higher density at sites 1 and 2 compared to site 3. This could be attributed to the greater preponderance of the pennate diatom (*Pseudo-nitzschia* cf. *delicatissima*) in May. The dominance of particular phytoplankton species, especially diatoms, is a rare phenomenon in the Saudi Arabian coastal waters of the Red Sea. However, it has been previously reported from the coastal waters of the northern Red Sea (Madkour et al. 2010; Devassy et al. 2017). In general, diatoms dominated in the phytoplankton community at sites 1 and 2 (88% and 71%, respectively), whereas the contribution of dinoflagellates at site 3 increased, accounting for approximately half of the community (53%). The isolation and shallowness of site 3, as well as water circulation may inhibit phytoplankton exchange with the two other sites. The presence of various microzooplankton species (personal observation) along with larger numbers of heterotrophic dinoflagellates at site 3 (33 species) clearly indicate the possible presence of a ‘microbial loop’ in the trophic structure. The minimal water exchange and the prolonged availability of high organic content in the water, possibly in terms of of bacterial origin, may have favored the growth of microzooplankton and heterotrophic dinoflagellates (Hansen 1991).

The number of phytoplankton species (220) recorded in the current study is comparable to that observed by Kürten et al. (2015) and Devassy et al. (2017) in the Saudi Arabian coastal waters of the Red Sea. However, it was much higher than in the coastal waters of Jeddah where 73 species were identified (Touliabah et al. 2010). Of the 533 phytoplankton species known from the entire Red Sea (Ismael 2015; Devassy et al. 2017; Abbas et al. 2018), only 220 species were observed in the present survey. This relatively small number of species may be due to the small area sampled. The slight dominance of diatoms over dinoflagellates may be due to favorable conditions in the region. The presence of the native phytoplankton genera (*Rhizosolenia*, *Chaetoceros*, *Tripos* and *Protoperidinium*) with varying numbers of species is consistent with previous observations (Dowidar et al. 1978; Kürten et al. 2015; Devassy et al. 2017; Al-Amri et al. 2020). In addition, the occurrence of native *Trichodesmium* sp. cyanophytes, especially in summer, suggests specific growth patterns of this genus in the Red Sea. The outbreak of *Trichodesmium* spp. during summer is a regular phenomenon in the Red Sea (Madkour et al. 2010; Kürten et al. 2015).

The Saudi Arabian coastal waters of the Red Sea are least known for the occurrence of potentially harmful species, mainly because of its oligotrophic nature. Recently, the situation in this particular ecosystem has been changing and the occurrence of potentially harmful bloom-causing phytoplankton, mainly dinoflagellates, is steadily increasing (Mohamed & Al-Shehri 2011; 2012; Kürten et al. 2015; Banguera-Hinestroza et al. 2016; Devassy et al. 2017; Al-Aidaroos et al. 2019). To date, none of the harmful species have caused an outbreak in the region, but there are still chances for possible future outbreaks, which could cause potential damage to the marine ecosystem by changing the environment. An example of these changes is the occurrence of the potentially harmful diatom species, *Pseudo-nitzschia* cf. *delicatissima*, in large numbers. Recently, Al-Aidaroos et al. (2019) studied the dominance of the same species in the coastal waters of Jeddah and explicitly listed it as a potentially harmful algal species from this environment in the near future. Furthermore, the occurrence of other 14 potentially harmful dinoflagellate species increases the likelihood of hazardous blooms in this area in the future.

5. Conclusion

The present study identifies a shifting pattern in the prevailing oligotrophic conditions of the Red Sea coastal waters. The major outcome of this study was the documentation of different phytoplankton species from the region, of which 21 diatom and four dinoflagellate species were considered as new records for the Red Sea. Another ecologically important aspect noted was the peculiar growth of the potentially harmful diatom species *Pseudo-nitzschia* cf. *delicatissima*. The higher density of this species observed in May was mainly due to the anthropogenic impact exerted on the system over a continuous period of time. Activities that alter the health status of the creek should be controlled and proper monitoring should be maintained in order to rejuvenate the system. Consequently, continuous monitoring of the coastal waters of the Red Sea is necessary to maintain a healthy ecosystem of ecological importance for the future generations.

Acknowledgements

This project was funded by the Deanship of Scientific Research (DSR) at King Abdulaziz University, Jeddah, Saudi Arabia, under the grant No. [G-462-150-40]. The authors, therefore, acknowledge with thanks DSR for technical and financial support. We extend our gratitude to Prof. Wafaaa Sallam for her critical reading of the manuscript and Mr. Reny P. Devassy for the assistance provided during the sampling process.

Author's contribution

MMS conceived the idea of the project. MMS, MAA and AAK carried out the sampling and the analysis. MMS wrote the initial manuscript, MAA and AAK provided suggestions and recommendations. The authors declare that there is no conflict of interest regarding the publication of this article.

References

Abbass, S.G., Madkour, F.F. & Abu-El-Regal, M.A. (2018) Checklist of phytoplankton species in the Egyptian Red Sea Coast of Hurghada. *Egypt. J. Aquat. Biol. & Fish.* 22: 93–101.

Acker, J., Leptoukh, G., Shen, S., Zhu, T. & Kempler, S. (2008). Remotely-sensed chlorophyll *a* observations of the northern Red Sea indicate seasonal variability and influence of coastal reefs. *J. Mar. Syst.* 69 (3): 191–204. DOI: 10.1016/j.jmarsys.2005.12.006.

Al-Aidaroos, A.M., Devassy, R.P. & El-Sherbiny, M.M. (2019). Unusual dominance of harmful microalgae *Pseudo-nitzschia delicatissima* cf. (Cleve) Heiden in the coastal waters of Jeddah, central Red Sea. *Pak. J. Bot.* 51(2): 1–6. DOI: 10.30848/PJB2019-2(44).

Al-Amri, A.A., Qari, H.A. & El-Sherbiny, M.M. (2020). Distribution and community structure of microphytoplankton in relation to increasing anthropogenic impact along coastal waters of Jeddah, the central Red Sea. *Oceanol. Hydrobiol. Stud.* 49(2): 193–205. DOI: 10.1515/ohs-2020-0018.

Al-Farawati, R. (2010). Environmental conditions of the coastal waters of Southern Corniche, Jeddah, Eastern Red Sea: Physico-chemical approach. *Aust. J. Basic Appl. Sci.* 4: 3324–3337.

Al-Harbi, S.M. & Affan, M. (2016). Seasonal dynamics of epiphytic microalgae and their host seaweeds Florideophyceae at Jeddah coast, the Red Sea, Saudi Arabia. *Pak. J. Bot.* 48(3): 1289–1298.

Alsaafani, M.A., Alraddadi, T.M. & Albarakati, A.M. (2017). Seasonal variability of hydrographic structure in Sharm Obhur and water exchange with the Red Sea. *Arab. J. Geosci.* 10(14): 315. DOI: 10.1007/s12517-017-3108-8.

Banguera-Hinestroza, E., Eikrem, W., Mansour, H., Solberg, I., Cúrdia, J. et al. (2016). Seasonality and toxin production of *Pyrodinium bahamense* in a Red Sea lagoon. *Harmful Algae* 55: 163–171. DOI: 10.1016/j.hal.2016.03.002.

Basaham, A.S. & El-Sayed, M.A. (2006). Sharm Obhur: environmental consequences of 20 years of uncontrolled coastal urbanization. *Marine Sciences* 17(1).

Basaham, A.S. & El-Shater, A. (1994). Textural and mineralogical characteristics of the surficial sediments of Sharm Obhur, Red Sea coast of Saudi Arabia. *Marine Sciences* 5(1).

Bastos, L., Bio, A. & Iglesias, I. (2016). The importance of marine observatories and of RAIA in particular. *Front. Mar. Sci.* 3: 140. DOI: 10.3389/fmars.2016.00140.

Brierley, A.S. & Kingsford, M.J. (2009). Impacts of climate change on marine organisms and ecosystems. *Curr. Biol.* 19(14): R602–R614. DOI: 10.1016/j.cub.2009.05.046.

Clarke, K.R. & Gorley, R.N. (2006). PRIMER v6: User Manual/Tutorial. PRIMER-E, Plymouth.

Devassy, R.P., El-Sherbiny, M.M., Al-Sofyani, A.M. & Al-Aidaroos, A.M. (2017). Spatial variation in the phytoplankton standing stock and diversity in relation to the prevailing environmental conditions along the Saudi Arabian coast of the northern Red Sea. *Mar. Biodivers.* 47: 995–1008. DOI: 10.1007/s12526-017-0693-4.

Devassy, R.P., El-Sherbiny, M.M., Al-Sofyani, A.A., Crosby, M.P. & Al-Aidaroos, A.M. (2019). Seasonality and latitudinal variability in the diatom-cyanobacteria symbiotic relationships in the coastal waters of the Red Sea, Saudi Arabia. *Symbiosis* 78(3): 215–227.

Dowidar, N.M. (1983). The genus *Ceratium* from the Red Sea. *J. Fac. Mar. Sci.* 3: 5–37.

Dowidar, N., Raheem El-Din, S. & Aleem, A. (1978). Phytoplankton populations in the region of Obhur, Jeddah, Saudi Arabia. *Bull. Fac. Sci., KAU* 2: 271–292.

Edwards, F.J. (1987). Climate and oceanography. *Red Sea* 1: 45–68.

El-Sayed, M.A. (2002). Nitrogen and phosphorus in the effluent of a sewage treatment site on the eastern Red Sea coast: daily cycle, flux and impact on the coastal area. *Int. J. Environ. Stud.* 59(1): 73–94. DOI: 10.1080/00207230211959.

Gómez, F. (2013). Reinstatement of the dinoflagellate genus *Tripos* to replace *Neoceratium*, marine species of *Ceratium* (Dinophyceae, Alveolata). *CICIMAR Oceánides* 28: 1–22.

Hallegraeff, G.M. (2003). Harmful algal blooms: a global overview, Manual on harmful marine microalgae 33: 1–22.

Halpern, B.S., Walbridge, S., Selkoe, K.A., Kappel, C.V., Micheli, F. et al. (2008). A global map of human impact on marine ecosystems. *Science* 319: 948–952. DOI: 10.1126/science.1149345.

Hansen, P.J. (1991). Quantitative importance and trophic role of heterotrophic dinoflagellates in a coastal pelagic food web. *Mar. Ecol. Prog. Ser.* 73(2–3): 253–261.

Ismael, A.A. (2015). Phytoplankton of the Red Sea. In R. Najeeb, & I.C.F. Stewart (Eds.), *The Red Sea: the formation, morphology, oceanography and environment of a young ocean basin* (pp. 567–583). Springer: Berlin Heidelberg.

Kürten, B., Al-Aidaroos, A.M., Kürten, S., El-Sherbiny, M.M., Devassy, R.P. et al. (2016). Carbon and nitrogen stable isotope ratios of pelagic zooplankton elucidate ecohydrographic features in the oligotrophic Red Sea. *Prog. Oceanogr.* 140: 69–90. DOI: 10.1016/j.pocean.2015.11.003.

Kürten, B., Khomayis, H.S., Devassy, R., Audritz, S., Sommer, U. et al. (2015). Ecohydrographic constraints on biodiversity and distribution of phytoplankton and zooplankton in coral reefs of the Red Sea, Saudi Arabia. *Mar. Ecol.* 36(4): 1195–1214. DOI: 10.1111/maec.12224.

LeGresley, M. & McDermott, G. (2010). *Counting chamber methods for quantitative phytoplankton analysis-haemocytometer, Palmer-Maloney cell and Sedgewick-Rafter cell.* UNESCO (IOC Manuals and Guides, no 55) (IOC/2010/MG/55): 25–30.

Li, W., El-Askary, H., ManiKandan, K.P., Qurban, M.A., Garay, M.J. et al. (2017). Synergistic use of remote sensing and modeling to assess an anomalously high chlorophyll-*a* event during summer 2015 in the south central Red Sea. *Remote Sens.* 9(8): 778. DOI: 10.3390/rs9080778.

Madkour, F.F., El-Sherbiny M.M. & Aamer, M.A. (2010). Phytoplankton population along certain Egyptian coastal regions of the Red Sea. *Egypt. J. Aquat. Biol. & Fish.* 14(2): 95–109.

Mohamed, Z.A. & Al-Shehri, A.M. (2011). Occurrence and germination of dinoflagellate cysts in surface sediments from the Red Sea off the coasts of Saudi Arabia. *Oceanologia* 53(1): 121–136. DOI: 10.5697/oc.53-1.121.

Mohamed, Z.A. & Al-Shehri, A.M. (2012). The link between shrimp farm runoff and blooms of toxic *Heterosigma akashiwo* in Red Sea coastal waters. *Oceanologia* 54(2): 287–309. DOI: 10.5697/oc.54-2.287.

Mudarris, M.S.A. & Turki, A.J. (2006). Sewage water quality and its dilution in the coastal waters of South Corniche, Jeddah, Red Sea. *JKAU: Met. Env. and Arid Land Agric. Sci.* 17: 115–128.

Parsons, T.R., Maita, Y. & Lalli, C.M. (1984). *A manual of chemical and biological methods for seawater analysis.* Pergamon Press, Oxford.

Peña-García, D., Ladwig, N., Turki, A.J. & Mudarris, M.S. (2014). Input and dispersion of nutrients from the Jeddah Metropolitan Area, Red Sea. *Mari. Poll. Bull.* 80(1): 41–51. DOI: 10.1016/j.marpolbul.2014.01.052.

Qurban, M.A., Balala, A.C., Kumar, S., Bhavya, P.S. & Wafar, M. (2014). Primary production in the northern Red Sea. *J. Mar. Syst.* 132: 75–82. DOI: 10.1016/j.jmarsys.2014.01.006.

Racault, M.F., Raitsos, D.E., Berumen, M.L., Brewin, R.J., Platt, T. et al. (2015). Phytoplankton phenology indices in coral reef ecosystems: Application to ocean-colour observations in the Red Sea. *Remote Sens. Environ.* 160: 222–234. DOI: 10.1016/j.rse.2015.01.019.

Shaikh, E.A., Roff, J.C. & Dowidar, N.M. (1986). Phytoplankton ecology and production in the Red Sea off Jiddah, Saudi Arabia. *Mar. Biol.* 92(3): 405–416.

Taylor, F.J.R. (1976). Dinoflagellates from the International Indian Ocean Expedition. A report on material collected by the R.V. "Anton Bruun" 1963-1964. *Bibl. Bot.* 132: 1–234.

Tomas, C.R. (1997). *Identifying Marine Phytoplankton*. UNESCO. Protocols for the joint global ocean flux study (JGOFS), Manual and Guides 29, Academic press, USA.

Touliabah, H.E., Abu El-Kheir, W.S., Kuchari, M.G. & Abdulwass, N.I.H. (2010). Phytoplankton composition at Jeddah Coast-Red Sea, Saudi Arabia in relation to some ecological factors. *JKAU: Mari. Sci.* 22 (1): 115–131.

Wafar, M., Qurban, M.A., Ashraf, M., Manikandan, K.P., Flandez, A.V. et al. (2016). Patterns of distribution of inorganic nutrients in Red Sea and their implications to primary production. *J. Mar. Syst.* 156: 86–98. DOI: 10.1016/j.jmarsys.2015.12.003.

Supplementary material 1

List of different phytoplankton species observed at the three sites during the study period. [– indicates the absence, + indicates the presence of a given species ($< 1 \times 10^3$ individuals m^{-3}), ++ indicates moderate cell abundance (10 to 100×10^3 individuals m^{-3}) and +++ indicates high cell abundance ($> 900 \times 10^3$ individuals m^{-3})].

	Site 1	Site 2	Site 3
Bacillariophyceae Centric diatoms			
Bacteriastrum hyalinum Lauder, 1864	—	—	+
Bellerochea horologicalis Stosch, 1980	—	+	—
Cerataulina sp.	+	+	—
Cerataulina bicornis (Ehrenberg) Hasle, 1985	+	+	+
Cerataulina dentate Hasle in Hasle & Syvertsen, 1980	+	+	+
Cerataulina pelagica (Cleve) Hendey, 1937	—	+	—
Chaetoceros sp.	+	+	+
Chaetoceros affinis Lauder, 1864	+	+	+
Chaetoceros coarctatus Lauder, 1864	—	+	—
Chaetoceros concavicornis Mangin, 1917	+	+	+
*Chaetoceros constrictus** Gran, 1897	+	—	—
*Chaetoceros costatus** Pavillard, 1911	—	+	—
Chaetoceros criophilus Castracane, 1886	—	—	+
Chaetoceros curvisetus Cleve, 1889	+	+	+
*Chaetoceros debilis** Cleve, 1894	—	—	+
Chaetoceros decipiens Cleve, 1873	+	+	+
Chaetoceros dichaeta Ehrenberg, 1844	—	+	—
*Chaetoceros eibenii** Grunow, 1882	+	+	+
Chaetoceros lorenzianus Grunow, 1863	+	—	—
*Chaetoceros mitra** (Bailey) Cleve, 1896	+	—	—
Chaetoceros peruvianus Brightwell, 1856	+	+	—
Chaetoceros pseudocurvisetus Mangin, 1910	—	+	—
Climacodium frauenfeldianum Grunow, 1868	—	+	—
*Corethron pennatum** (Grunow) Ostenfeld, 1909	—	—	+
Coscinodiscus sp.	+	—	+
Coscinodiscus granii Gough, 1905	+	+	—
Coscinodiscus marginatus Ehrenberg, 1844	+	+	—
Coscinodiscus radiates Ehrenberg, 1840	+	+	+
Dactyliosolen sp.	—	+	—
Dactyliosolen fragilissimus (Bergon) Hasle, 1996	+	+	+
*Dactyliosolen phuketensis** (B.G.Sundström) G.R.Hasle, 1996	+	+	+
Detonula pumila (Castracane) Gran, 1900	+	+	+
Ditylum brightwellii (T.West) Grunow, 1885	—	+	—
*Ethmodiscus rex** (Wallich in Rattray) Hendey in Wiseman & Hendey, 1953	+	+	—
Eucampia zodiacus Ehrenberg, 1839	+	+	—
Guinardia sp.	+	—	—
Guinardia cylindrus (Cleve) Hasle, 1996	+	+	+
Guinardia delicatula (Cleve) Hasle, 1997	+	+	+
Guinardia flaccida (Castracane) H.Peragallo, 1892	+	+	+
Guinardia striata (Stolterfoth) Hasle, 1996	+	+	+
Helicotheca tamesis (Shrubsole) M.Ricard, 1987	—	+	—
Hemiaulus hauckii Grunow ex Van Heurck, 1882	+	+	+
Hemiaulus membranaceus Cleve	+	+	+
Hemiaulus sinensis Greville, 1865	+	+	+
Hemidiscus cuneiformis Wallich, 1860	+	—	+
Lauderia annulata Cleve, 1873	+	+	+
Leptocylindrus danicus Cleve, 1889	+	+	+

	Site 1	Site 2	Site 3
*Leptocylindrus minimus** Gran, 1915	+	+	+
Lithodesmium undulatum Ehrenberg, 1839	+	+	+
Odontella aurita (Lyngbye) *C.Agardh, 1832*	—	+	—
Paralia sulcate (Ehrenberg) Cleve, 1873	+	+	—
Planktoniella sol (C.G.Wallich) Schütt, 1892	+	+	—
Proboscia alata (Brightwell) Sundström, 1986	+	++	+
*Pseudoguinardia recta** von Stosch, 1986	+	+	+
Pseudosolenia calcar-avis (Schultze) B.G.Sundström, 1986	+	+	+
Rhizosolenia sp.	—	—	+
Rhizosolenia acicularis B.G.Sundström, 1986	—	+	+
Rhizosolenia acuminate (H.Peragallo) H.Peragallo, 1907	—	+	—
Rhizosolenia bergonii H.Peragallo, 1892	+	—	—
*Rhizosolenia castracanei** H.Peragallo, 1888	—	—	+
*Rhizosolenia clevei** Ostenfeld, 1902	+	+	+
*Rhizosolenia crassa** Schimper, 1905	+	—	—
*Rhizosolenia curvata** Zacharias, 1905	+	+	+
*Rhizosolenia formosa** H.Peragallo, 1888	+	+	—
Rhizosolenia hebetate Bailey, 1856	+	+	+
Rhizosolenia imbricate Brightwell, 1858	+	+	+
Rhizosolenia ostenfeldii B.G.Sundström, 1986	—	+	—
*Rhizosolenia polydactyla** Castracane, 1886	+	+	—
Rhizosolenia setigera Brightwell, 1858	+	+	+
*Rhizosolenia striata** Greville, 1864	—	+	—
Rhizosolenia styliformis T.Brightwell, 1858	+	+	+
Rhizosolenia temperei H.Peragallo, 1888	—	+	—
Skeletonema costatum (Greville) Cleve, 1873	+	+	+
Thalassiosira sp.	+	+	—
Thalassiosira subtilis (Ostenfeld) Gran, 1900	+	+	—
Triceratium dubium Brightwell, 1859	+	—	—
Pennate diatoms			
Entomoneis alata (Ehrenberg) Ehrenberg, 1845	+	+	+
Amphiprora gigantean Grunow, 1860	+	+	+
Amphora sp.	+	+	—
Asterionellopsis glacialis (Castracane) Round, 1990	+	++	+
Climacosphenia moniligera Ehrenberg, 1843	+	++	+
Cylindrotheca closterium (Ehrenberg) Reimann & J.C.Lewin, 1964	+	++	+
Diploneis smithii (Brébisson) Cleve, 1894	+	—	—
Fragilaria sp.	—	+	+
Fragilaria striatula Lyngbye, 1819	+	+	—
Gyrosigma fasciola (Ehrenberg) J.W.Griffith & Henfrey, 1856	+	+	+
Haslea trompii (Cleve) Simonsen, 1974	+	+	+
*Haslea wawrikae** (Hustedt) Simonsen, 1974	—	+	—
Licmophora abbreviate C.Agardh, 1831	+	+	+
Licmophora flabellata (Grev.)C.Agardh, 1831	+	+	—
Licmophora gracilis (Ehrenberg) Grunow, 1867	+	+	—
Lioloma elongatum (Grunow) Hasle, 1997	—	+	—
Meuniera membranacea (Cleve) P.C.Silva, 1996	+	+	+
Navicula sp.	+	+	—
Navicula directa (W.Smith) Ralfs, 1861	+	++	+
Navicula distans (W.Smith) Ralfs, 1861	—	+	—
Navicula transitans Cleve, 1883	+	+	+
Nitzschia sp.	+	+	+
*Nitzschia acicularis** (Kützing) W.Smith, 1853	+	—	—
Nitzschia longissimi (Brébisson) Ralfs, 1861	+	+	+

	Site 1	Site 2	Site 3
Petrodictyon gemma (Ehrenberg) D.G.Mann, 1990	—	—	—
Pleurosigma sp.	+	—	—
Pleurosigma directum Grunow, 1880	+	+	—
Pleurosigma elongatum W.Smith, 1852	+	+	+
Pleurosigma formosum W.Smith, 1852	+	+	—
Pleurosigma normanii Ralfs, 1861	—	—	+
Pseudo-nitzschia delicatissima$^{\odot}$ (Cleve) Heiden, 1928	+++	+++	+
Pseudo-nitzschia seriata$^{\odot}$ (Cleve) H.Peragallo, 1899	+	+	+
Striatella unipunctata (Lyngbye) C.Agardh, 1832	—	+	—
Synedra sp.	+	+	—
*Synedra biceps** W.Smith, 1853	+	—	—
*Synedropsis hyperborea** (Grunow) G.R.Hasle, L.K.Medlin & E.E.Syvertsen, 1994	+	—	—
Thalassionema bacillare (Heiden) Kolbe, 1955	+	+	—
Thalassionema frauenfeldii (Grunow) Tempère & Peragallo, 1910	+	+	—
Thalassionema nitzschioides (Grunow) Mereschkowsky, 1902	—	—	+
Thalassiothrix longissimi Cleve & Grunow, 1880	+	+	+
Toxarium undulatum Bailey, 1854	+	+	—
Dinophyceae			
Alexandrium sp.	+	+	+
Alexandrium affine (H.Inoue & Y.Fukuyo) Balech, 1995	—	+	+
Alexandrium fundyense$^{\odot}$ Balech, 1985	—	+	—
Alexandrium minutum$^{\odot}$ Halim, 1960	+	+	+
Alexandrium tamarense$^{\odot}$ (Lebour, 1925) Balech, 1995	+	+	+
Amphidinium sphenoides Wülff, 1916	—	+	—
Amphisolenia bidentate Schröder, 1900	—	+	—
Ceratocorys armata (Schütt) Kofoid, 1910	+	+	—
Ceratocorys horrida Stein, 1883	+	+	+
Corythodinium tesselatum (Stein) Loeblich Jr. & Loeblich III, 1966	+	—	+
Dinophysis sp.	+	+	+
Dinophysis acuminata$^{\odot}$Claparède & Lachmann, 1859	+	—	—
Dinophysis acuta$^{\odot}$Ehrenberg, 1839	+	—	—
Dinophysis caudata$^{\odot}$ Saville-Kent, 1881	+	++	++
Dinophysis dens Pavillard, 1915	+	—	—
Dinophysis hastate Stein, 1883	+	+	+
Dinophysis miles$^{\odot}$ Cleve, 1900	+	+	+
Dinophysis odiosa (Pavillard) Tai & Skogsberg, 1934	+	+	+
Dinophysis tripos$^{\odot}$ Gourret, 1883	+	++	+
Dinophysis uracantha Stein, 1883	+	+	—
Gonyaulax sp.	+	—	+
Gonyaulax polygramma Stein, 1883	+	+	+
Gonyaulax scrippsae Kofoid, 1911	+	—	—
Gonyaulax spinifera$^{\odot}$ (Claparède & Lachmann) Diesing, 1866	+	+	+
Gonyaulax verior Sournia, 1973	+	+	+
Gymnodinium sp.	—	+	—
Heterocapsa triquetra (Ehrenberg) Stein, 1883	—	—	+
*Ornithocercus heteroporus** Kofoid, 1907	+	—	—
Ornithocercus magnificus Stein, 1883	+	—	—
Ornithocercus quadratus Schütt, 1900	+	—	—
Ornithocercus splendidus Schütt, 1895	+	+	+
Ornithocercus steinii Schütt, 1900	+	—	—
*Ornithocercus thumii** (Schmidt) Kofoid & Skogsberg, 1928	+	+	+
Oxytoxum gracile Schiller, 1937	+	+	—
Phalacroma sp.	+	—	—
Phalacroma cuneus F.Schütt, 1895	+	+	—

	Site 1	Site 2	Site 3
Phalacroma doryphorum Stein, 1883	+	+	+
Phalacroma mitra$^{\odot}$ F.Schütt, 1895	+	—	—
*Phalacroma oxytoxoides** (Kofoid) F.Gomez, P.Lopez-Garcia & D.Moreira, 2011	—	—	+
Phalacroma rapa Jorgensen, 1923	+	—	—
Phalacroma rotundatum$^{\odot}$ (Claparéde & Lachmann) Kofoid & Michener, 1911	+	+	+
Podolampas palmipes Stein, 1883	—	+	—
Podolampas spinifera Okamura, 1912	—	+	—
Prorocentrum sp.	+	—	—
Prorocentrum cordatum$^{\odot}$ (Ostenfeld) J.D.Dodge, 1975	+	+	+
Prorocentrum gracile Schütt, 1895	+	+	+
Prorocentrum lima$^{\odot}$ (Ehrenberg) F.Stein, 1878	+	+	—
Prorocentrum micans$^{\odot}$ Ehrenberg, 1834	+	+	+
Prorocentrum triestinum J.Schiller, 1918	+	+	+
Protoceratium reticulatum (Claparède & Lachmann) Bütschli, 1885	—	+	—
Protoperidinium sp.	+	+	+
*Protoperidinium bipes** (Paulsen, 1904) Balech, 1974	+	+	+
Protoperidinium claudicans (Paulsen, 1907) Balech, 1974	+	+	+
Protoperidinium conicum (Gran, 1900) Balech, 1974 †	+	++	++
Protoperidinium crassipes (Kofoid, 1907) Balech, 1974	+	+	+
Protoperidinium curtipes (Jørgensen, 1912) Balech, 1974	—	—	+
Protoperidinium depressum (Bailey, 1854) Balech, 1974	—	+	+
Protoperidinium divergens (Ehrenberg, 1840) Balech, 1974	+	++	++
Protoperidinium elegans (Cleve, 1900) Balech, 1974	+	+	+
Protoperidinium grande (Kofoid, 1907) Balech, 1974	+	—	+
Protoperidinium leonis (Pavillard, 1916) Balech, 1974	—	+	+
Protoperidinium oblongum (Aurivillius) Parke & Dodge, 1976	+	—	—
Protoperidinium oceanicum (VanHöffen, 1897) Balech, 1974	+	+	+
Protoperidinium ovatum Pouchet, 1883	+	+	+
Protoperidinium ovum (Schiller, 1911) Balech, 1974	+	+	++
Protoperidinium pallidum (Ostenfeld, 1899) Balech, 1973	+	+	++
Protoperidinium pellucidum Bergh, 1881	+	+	+
Protoperidinium pentagonum (Gran, 1902) Balech, 1974	+	+	+
Protoperidinium steinii (Jørgensen, 1899) Balech, 1974	+	+	++
Pyrocystis lunula (Schütt) Schütt, 1896	+	—	—
Pyrophacus steinii (Schiller) Wall & Dale, 1971	—	+	+
Scrippsiella trochoidea (Stein) Loeblich III, 1976	+	—	+
Tripos arietinus (Cleve) F.Gómez, 2013	—	+	—
Tripos brevis (Ostenfeld & Johannes Schmidt) F.Gómez 2013	+	+	+
Tripos candelabrus (Ehrenberg) F.Gómez, 2013	+	+	—
Tripos carriensis (Gourret) F.Gómez, 2013	+	+	+
Tripos contortus (Gourret) F.Gómez, 2013	+	+	+
Tripos declinatus (G.Karsten) F.Gómez, 2013	+	+	+
Tripos deflexus (Kofoid) F.Gómez, 2014	+	+	—
Tripos furca (Ehrenberg) F.Gómez, 2013	+	++	++
Tripos fusus (Ehrenberg) F.Gómez 2013	+	++	++
Tripos gibberus (Gourret) F.Gómez 2013	+	+	—
Tripos horridus (Cleve) F.Gómez 2013	+	++	+
Tripos incisus (Karsten) F.Gómez, 2013	—	+	+
Tripos inflatus (Kofoid) F.Gómez 2013	+	+	+
Tripos kofoidii (Jörgenen) F.Gómez, 2013	—	+	—
Tripos lineatus (Ehrenberg) F.Gómez, 2013	+	++	+
Tripos longipes (J.W.Bailey) F.Gómez, 2013	+	+	—
Tripos lunula (Schimper ex Karsten) F.Gómez, 2013	+	+	+
Tripos macroceros (Ehrenberg) F.Gómez, 2013	+	+	+

	Site 1	Site 2	Site 3
Tripos pentagonus (Gourret) F.Gómez, 2013	+	+	—
Tripos platycornis (Daday) F.Gómez 2013	+	—	—
Tripos praelongus (Lemmermann) Gómez, 2013	—	—	+
Tripos pulchellus (Schröder) F.Gómez, 2013	+	+	+
Tripos ranipes (Cleve) F.Gómez, 2013	+	+	—
Tripos symmetricus (Pavillard) F.Gómez 2013	+	+	+
Tripos teres (Kofoid) F.Gómez 2013	+	++	+
Tripos trichoceros (Ehrenberg) Gómez 2013	+	+	+
Tripos vultur (Cleve) F.Gómez, 2013	+	+	+
Cyanophyceae			
Anabaena sp.	—	+	—
Nostoc sp.	—	+	—
Richelia intracellularis J.Schmidt, 1901	+	+	+
Trichodesmium sp.	++	++	+

*New record for the Red Sea, ʘ Harmful algal species